Photodissociation Dynamics of *N*-Methylindole, *N*-Methylpyrrole, and Anisole†

Chien-Ming Tseng,‡ Yuan T. Lee,‡ and Chi-Kung Ni*,§

Institute of Atomic and Molecular Sciences, Academia Sinica, P.O. Box 23-166, Taipei, 10617 Taiwan

Received: November 13, 2008; Revised Manuscript Received: December 25, 2008

Photodissociation experiments employing molecular beams of *N*-methylindole, *N*-methylpyrrole, and anisole at 193 and 248 nm, respectively, have been conducted using multimass ion imaging techniques. We find that CH_3 elimination is the sole dissociation channel for the studied molecules at both 193 and 248 nm. The photofragment translational energy distribution of anisole is found to contain both fast and slow components at the two wavelengths. On the other hand, a fast component (large recoil velocity) is dominant for *N*-methylindole at 248 nm, and a slow component (small recoil velocity) is dominant at 193 nm. The absorption coefficient of *N*-methylpyrrole is too weak for study at 248 nm. The photofragment translational energy distribution at 193 nm includes a large portion of the slow component and a small portion of the fast component. The findings indicate that the fast component corresponds to dissociation from the repulsive excited state and the slow component corresponding to dissociation from the ground electronic state. A comparison with the photodissociation dynamics of phenol, pyrrole, and indole suggests that replacement of the H atom by CH_3 does not change the dissociation channels on the excited state. However, the respective dissociation channels for anisole and *N*-methylpyrrole on the ground state differ significantly from that for phenol and pyrrole.

I. Introduction

One important photophysical characteristic of aromatic biomolecules concerns the low fluorescence quantum yields upon excitation by ultraviolet (UV) light.[1−4] This behavior indicates the presence of a fast nonradiative channel, which efficiently quenches the fluorescence. This nonradiative process is assumed to be ultrafast internal conversions (IC) to the ground electronic state. The so-called "photostability" of these aromatic biomolecules prevents undesirable photochemical reactions from occurring after UV irradiation.[2,3] However, recent theoretical calculations indicate that the $1\pi\sigma^*$ excited electronic state plays a crucial role in the photochemistry of these molecules, in particular, those molecules containing hydroxy and azine groups such as phenol, indole, and pyrrole.[5] For indole, the first excited $1\pi\pi^*$ state is bound with respect to the N−H bond distance, whereas the $1\pi\sigma^*$ state is repulsive. The diabatic $1\pi\sigma^*$ potential curve correlates with ground-state products: C_8NH_6 + H. Although absorption of UV photons corresponds to excitation to the $1\pi\pi^*$ state, its population can be transferred to the $1\pi\sigma^*$ potential through a conical intersection. As a result, instead of direct internal conversion to the ground state, dissociation from the $1\pi\sigma^*$ potential curve offers an alternative explanation for the rapid fluorescence quenching. Repulsive potential energy surfaces for $1\pi\sigma^*$ are also available for phenol along its O−H bond and for pyrrole along its N−H bond. The difference is that the respective $1\pi\pi^*$ potential minima for indole and phenol fall below that of the $1\pi\sigma^*$ potential energy surface (in the area close to the equilibrium geometry in the ground electronic state) in contrast to pyrrole, where the $1\pi\sigma^*$ state is lowest in energy.

Experimental evidence in support of these theoretical calculations was available years earlier and more recently. Photofragment translational spectroscopy has been used to study the photodissociation of pyrrole at 193 and 248 nm under collision-free conditions. In addition to some ring-opening dissociation channels, cleavage of the N−H bond on the repulsive electronically excited state of pyrrole was observed before the theoretical predictions.[6] Recent H atom photofragment velocity map ion imaging and Rydberg H atom high-resolution translational spectroscopy have uncovered more detailed information on the H atom elimination channel in support of the previous experimental measurements.[7] Hydrogen atom elimination on the repulsive excited states of phenol and indole was first observed in multimass ion imaging/molecular beam experiments.[8,9] More recently, Rydberg H atom high-resolution translational spectroscopy has revealed a detailed dissociation mechanism and a vibrational mode dependence for this process.[10]

The dissociation mechanism may change if hydrogen atoms are replaced methyl groups. For example, differences in delayed luminescence between *N*-methylindole and indole in the gas phase using laser irradiation wavelengths of 266 nm and 230−250 nm have been reported.[11] Delayed annihilation fluorescence, which spectrally matches fast fluorescence, was observed for *N*-methylindole; however, there is no similar fluorescence with indole. Rather, a delayed luminescence band with a wavelength maximum of 535 nm was observed, which was interpreted as free-radical luminescence resulting from N−H bond dissociation for indole. Interestingly, no free radicals from the dissociation of the N−C bond in *N*-methylindole have been observed.

On the other hand, anisole and phenol appear to have similar dissociation mechanisms in the gas phase. The photodissociation of gaseous anisole has been studied at 193 nm.[12] Transient absorption spectra (in the range 210−300 nm) show two broad bands, assigned to phenoxyl radicals, which are produced on a time scale shorter than 1 ns upon irradiation by an ArF laser. The photodissociation mechanism was a proposed predissociation. By contrast, both phenoxyl and phenoxymethyl radicals,

* Corresponding author. E-mail: ckni@po.iams.sinica.edu.tw.

† Part of the "George C. Schatz Festschrift".

‡ Also at Department of Chemistry, National Taiwan University, Taipei, Taiwan.

§ Also at Department of Chemistry, National Tsing Hua University, Hsinchu, Taiwan.

10.1021/jp8100305 CCC: $40.75
Published on Web 01/26/2009

were observed in the transient absorption spectra of anisole (in acetonitrile) at 248 nm in laser photolysis experiments.[13]

The photophysics of jet-cooled *N*-methylpyrrole molecules following excitation to the first excited singlet state (242.7−237 nm) has been investigated by the resonance enhanced multiphoton ionization spectroscopy/velocity map ion imaging of CH_3 photoproducts.[14] Direct dissociation on the repulsive excited potential energy surface yields fast CH_3 fragments. However, this product channel was only observed within a narrow wavelength range near the absorption band origin. Slow CH_3 fragments were observed (at all of the photolysis wavelengths used) and are attributed to the dissociation of highly vibrationally excited molecules in the ground state formed via radiationless transfer from the excited electronic state.

In this work, we investigated the photodissociation of *N*-methylindole, *N*-methylpyrrole, and anisole at 193 and 248 nm, respectively, using multimass ion imaging techniques, and we compare our findings with the previous studies.

II. Experiment

Our experiments have been described in detail elsewhere.[14] Here, we offer a brief description. Each compound tested is vaporized by flowing ultrapure He (400 Torr) through a reservoir filled with a solid sample of the compound at $T = 50$ °C. The compound/He mixture is then expanded through an 800 μm (nozzle diameter), high-temperature (70 °C) pulsed nozzle to form the molecular beam. Molecules in the beam are photodissociated by a UV photolysis laser pulse (Lambda Physik Compex 205: pulse duration ~ 20 ns). The photofragments are distributed on an expanding sphere (due to the recoil velocity) in flight to the ionization region (due to the molecular beam velocity, or center-of-mass velocity) where they are ionized by a VUV laser pulse. The distance and time delay between the VUV laser and the photolysis laser pulses are set so that the VUV laser beam passes through the center-of-mass of the dissociation products, generating photofragment ions along the VUV beam. The length of the ion segment is proportional to the fragment recoil velocity (in the center-of-mass frame) multiplied by the delay time between the photolysis and the ionization laser pulses. To separate the different masses within an ion segment, a pulsed electric field is used to extract the ions into a mass spectrometer. With the mass analysis conducted in the mass spectrometer, the length of each fragment ion segment continues to expand in its original direction in accordance with the recoil velocity. At the exit port of the mass spectrometer, a two-dimensional ion detector is used to detect ion positions and intensity distributions. In this two-dimensional detector, one direction is the recoil velocity axis, and the other is the mass axis.

Dependent on the molecular beam velocity, changes in the distance, between the photolysis and the VUV laser beams, are made to match the delay time between the two laser pulses to ensure that the ionization laser passes through the center-of-mass of the products. Changing the distance between the two laser beams changes the length of the fragment ion segment in the images we observe. Molecules that do not dissociate into fragments upon absorption of UV photons contain high internal energies. These hot molecules, which remain within the molecular beam, move with the beam velocity to the ionization region where they are ionized by the VUV laser. The wavelength of the VUV laser in this experiment was set at 118.2 nm. The resulting photon energy was high enough to ionize the parent molecules. The dissociation of parent molecular cations would not occur with the energy left after the VUV laser ionization.

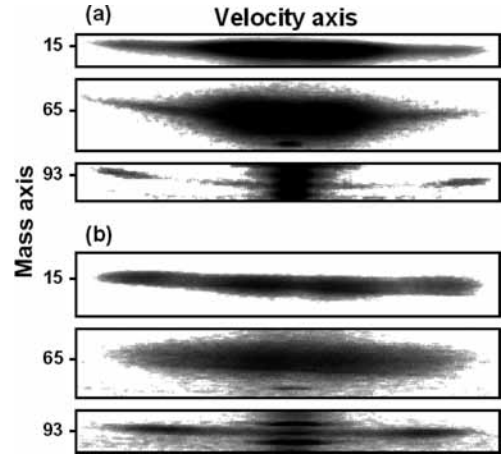

Figure 1. Photofragment ion images of anisole at photolysis wavelength (a) 193 nm with pump−probe delay time 0.7, 15, and 15 μs for $m/e = 15$, 65, and 93, respectively; (b) 248 nm with pump−probe delay time 2, 14, and 14 μs for $m/e = 15$, 65, and 93, respectively. The ionization wavelength is 118 nm.

However, the VUV laser photons are sufficiently energetic to dissociate the hot molecules. The resulting ion image for dissociative ionization differs from that for the dissociation products of the neutral parent molecules. Because ionization and dissociation occur at the same position in space, the image for dissociative ionization is a two-dimensional projection of the photofragment ion's three-dimensional recoil velocity distribution. It is a disk-like image, rather than a line-shape image. Additionally, the size of the image from dissociative ionization does not change with the delay time.

On the other hand, if the fragments crack into small ionic fragments upon VUV photoionization, the shape of the image is also disk-like; however, the width of the image changes with the delay time. From the shape of the image, along with changes in its width (with respect to the delay time), the images resulting from the dissociation of neutral molecules can clearly be distinguished from those images resulting from the cracking of heavy fragments and the dissociative ionization of parent molecules.

III. Results and Discussion

A.. Anisole. Figure 1 depicts the photofragment ion images obtained from the photodissociation of anisole at 193 nm. Fragments of charge-to-mass ratios $m/e = 93$, 65, and 15 were observed. Examination of the photolysis laser power dependence in the range 0.15−0.87 mJ/cm^2 showed that the fragments were from one-photon dissociation. The fragments with charge-to-mass ratios $m/e = 93$ and 15, correspond to C_6H_5O and CH_3 radicals from C−O bond cleavage: $C_6H_5OCH_3 \rightarrow C_6H_5O$ ($m = 93$) + CH_3 ($m = 15$). The image for fragment $m/e = 65$ is disk-like, but the width of the image changes with the delay time. The image is a product of the dissociative ionization of phenoxyl radical by VUV photoionization (due to the excess VUV photon energy): $C_6H_5O + h\nu$ (118 nm) → $C_5H_5^+$ ($m/e = 65$) + CO. This cracking pattern has also been observed in the photoionization of phenoxyl radical as generated from the photodissociation of phenol.[15] A comparison of the momentum distributions for CH_3 ($m/e = 15$) and the sum of C_6H_5O ($m/e = 93$) and $C_5H_5^+$ ($m/e = 65$) confirms this dissociation channel. The photodissociation of anisole at 248 nm shows the same dissociation channel and fragment-cracking pattern. The photolysis laser power dependence in the range 2.1−17.6 mJ/cm^2 confirmed a one-photon dissociation. Translational energy

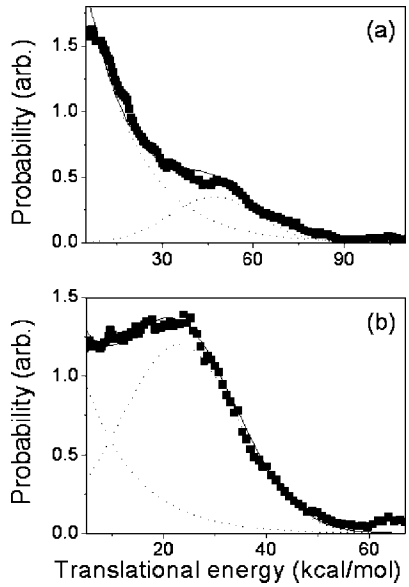

Figure 2. Photofragment translational energy distributions of reaction $C_6H_5OCH_3 \rightarrow C_6H_5O + CH_3$ at (a) 193 nm and (b) 248 nm.

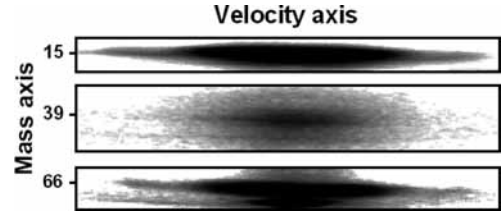

Figure 3. Photofragment ion images of *N*-methylpyrrole at photolysis wavelength 193 nm with pump−probe delay time 0.3, 10, and 8 μs for m/e = 15, 39, and 66, respectively.

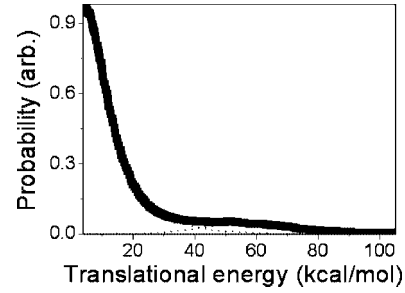

Figure 4. Photofragment translational energy distribution of reaction $C_4NH_4CH_3 \rightarrow C_4NH_4 + CH_3$ at 193 nm.

distributions for the CH_3 elimination channel at 193 and 248 nm are illustrated in Figure 2a,b. The distribution can be attributed to the sum of two components: slow and fast (i.e., slow and fast fragment recoil velocities). The probability for the slow component decreases monotonically with increasing translational energy and the peak for the fast component, far from zero, finds its distribution reaching the maximum value for the available energy (for $C_6H_5OCH_3 \rightarrow C_6H_5O + CH_3$, the heat of reaction is 64 kcal/mol). Available energies are 84 and 51 kcal/mol for 193 and 248 nm, respectively. The slow component (small recoil velocity) is characteristic of dissociation from a molecule that undergoes internal conversion to the ground electronic state with little or no exit barrier. The fast component (large recoil velocity) is typical for dissociation from a repulsive excited state or dissociation from an electronic state with a large exit barrier.

The photodissociation of phenol at 193 and 248 nm has been examined using multimass ion-imaging techniques and step-scan time-resolved Fourier-transform spectroscopy.[15] Major dissociation channels at 193 nm include cleavage of the O−H bond, elimination of CO, and elimination of H_2O. Only the elimination of CO and H_2O are observed at 248 nm. The translational energy distribution shows that H atom elimination occurs in both the excited and the ground electronic states, but elimination of CO or H_2O occurs only in the ground state.

Comparisons made between anisole and phenol show similarities and differences. Dissociation on the repulsive excited state is observed with both molecules. This indicates that the properties of the repulsive excited $\pi\sigma^*$ state and the coupling between the bound state and the $\pi\sigma^*$ state do not change significantly as the H atom in the hydroxy group is replaced by a CH_3 group. Dissociation from the repulsive state remains as one of the major channels. The only dissociation channel for anisole on the ground state is CH_3 elimination. By contrast, phenol exhibits various dissociation channels on the ground state. The $C_6H_5O-CH_3$ bond energy (64 kcal/mol) is smaller than the C_6H_5O-H bond energy (88 kcal/mol), which is one reason why O−C bond cleavage is the dominant channel for anisole on the ground state. Another reason is that the migration of the H atom from the hydroxy group to the aromatic ring is the first step for the CO elimination channel in phenol. The corresponding step for anisole becomes CH_3 migration, which is unlikely due to the large barrier height. As a consequence, CH_3 elimination is the only dissociation channel for anisole on the ground state.

B. *N*-Methylpyrrole. The absorption coefficient for *N*-methylpyrrole at 248 nm is too small for our purposes.[16] Therefore, our photodissociation experiments for *N*-methylpyrrole were at 193 nm. Figure 3 illustrates the photofragment ion images obtained from the photodissociation of *N*-methylpyrrole at 193 nm. Fragments of m/e = 66, 39, and 15 were observed. Examination of the photolysis laser power dependence in the region of 0.08−0.67 mJ/cm^2 indicates that the fragments are from one-photon dissociation. Photofragments of m = 66 and 15 correspond to C_4NH_4 and CH_3 radicals from N−C bond cleavage: $C_4NH_4CH_3 \rightarrow C_4NH_4$ (m = 66) + CH_3 (m = 15). The image of fragment m/e = 39 is disk-like, and the width changes with the pump−probe delay time. The image corresponds to the dissociative ionization of pyrrole radical by VUV photoionization due to the excess VUV photon energy: $C_4NH_4 + h\nu(118\text{nm}) \rightarrow C_3H_3^+$ (m/e = 39) + HCN. The translational energy distribution of this channel is shown in Figure 4. It includes a large portion of the slow component and a small portion of the fast component.

Photofragment translational energy spectroscopy has been used to study the photodissociation of pyrrole at 193 nm under collision-free conditions.[6] Five primary dissociation channels were observed. Two channels result from cleavage of the N−H bond, with one channel following internal conversion to the ground state and the other channel originating from electronically excited pyrrole. Another two dissociation channels are involved in HCN elimination with one channel producing vinylmethylene and the other channel creating cyclopropene. The final channel concerns internal conversion to the ground state followed by a ring opening and N−C bond cleavage to form NH + C_4H_4.

No similar ring-opening dissociation channel was observed in *N*-methylpyrrole, only cleavage of the N−C bond, the majority of which resulted from internal conversion to the ground state and to a lesser extent from the electronically excited state. The reason that there are no analogous ring-opening

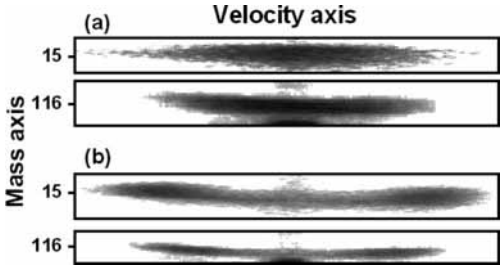

Figure 5. Photofragment ion images of *N*-methylindole at photolysis wavelength (a) 193 nm with pump−probe delay time 3 and 19 μs for $m/e = 15$ and 116; (b) 248 nm with pump−probe delay time 2 and 20 μs for $m/e = 15$ and 116, respectively.

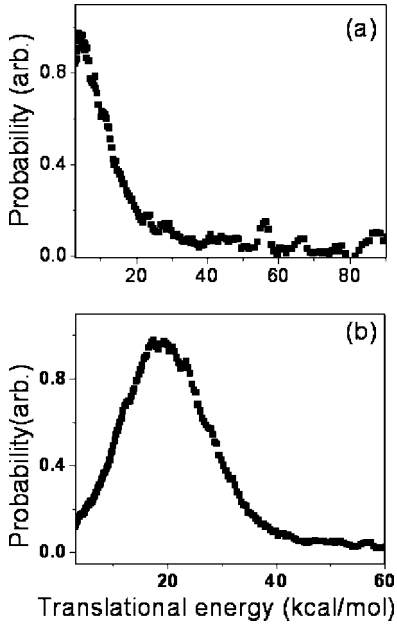

Figure 6. Photofragment translational energy distributions of reaction $C_8NH_6CH_3 \rightarrow C_8NH_6 + CH_3$ at (a) 193 nm and (b) 248 nm.

dissociation channels is similar to that for phenol and anisole. Ring-opening dissociation in pyrrole requires migration of the H atom from the N−H group to initiate the process. Replacement of the H atom by the CH_3 group simply hinders the first step, and consequently no ring-opening dissociation channels occur. Previous studies in the region of 242.7−237 nm show that dissociation from the excited state was only observed in a narrow wavelength range near the absorption band origin.[14] Our results extend to shorter wavelengths and we find that dissociation from the excited state can still be observed at 193 nm, although it is a minor channel.

C. *N*-Methylindole. Fragments of $m/e = 116$ and 15 were observed from the photodissociation of *N*-methylindole at 193 nm. Figure 5 illustrates the photofragment ion images. A study of the photolysis laser power dependence in the region of 0.1−0.67 mJ/cm^2 showed that the fragments were from one-photon dissociation. A match of the momentum distributions for the two fragments suggests that they come from the same dissociation channel: $C_8NH_6CH_3 \rightarrow C_8NH_6$ ($m = 116$) + CH_3 ($m = 15$). The photofragment translational energy distribution of this channel is illustrated in Figure 6a. Photodissociation of *N*-methylindole at 248 nm reveals the same dissociation channel. The photolysis laser power dependence measured in the region of 0.82 −6.9 mJ/cm^2 showed that they were from one-photon dissociation. The translational energy distribution obtained at 248 nm is given in Figure 6b. The translational energy distributions at these two wavelengths illustrate very different results. The fast component is the major component in the translational energy distribution at 248 nm. However, it is barely observed at 193 nm. The results indicate dissociation mechanisms that differ at these two wavelengths.

Photodissociation of indole at 193 and 248 nm under collision-free conditions has been studied using these same techniques. Hydrogen atom elimination was found to be the sole dissociation channel at both wavelengths. The photofragment translational energy distribution obtained at 193 nm contains both a fast and a slow component. Approximately 54% of indole molecules (following photoexcitation at 193 nm) dissociate from the electronically excited state, resulting in the fast component. The remaining percentage of indole dissociates through the ground electronic state, giving rise to the slow component. Similarly, a two-component translational energy distribution was observed at 248 nm. However, more than 80% of indole dissociates from the electronically excited-state after absorption of 248 nm photons.

A comparison of indole and *N*-methylindole shows similar wavelength dependence in the competition between dissociation on the ground state and dissociation on the repulsive excited state. With decreasing pump laser photon energy, internal conversion to the ground state becomes less important. Population transfer from the excited bound state to the repulsive excited state becomes the dominant channel at 248 nm. However, unlike that for indole, dissociation from the excited state at 193 nm rarely occurs for *N*-methylindole. Our findings are in contrast to conclusions drawn from delayed luminescence investigations of *N*-methylindole and indole, suggesting that C−C bond cleavage does not occur at the photolysis wavelengths 230−250 and 266 nm.[11]

Acknowledgment. The work was supported by the National Science Council Taiwan, under Contract No. NSC 96-2113-M-001-029.

References and Notes

(1) Robin, M. B. *Higher Excited States of Polyatomic Molecules*; Academic: New York, 1972.
(2) Callis, P. R. *Annu. Rev. Phys. Chem.* **1983**, *34*, 329.
(3) Creed, D. *Photochem. Photobiol.* **1984**, *39*, 537.
(4) Crespo-Hernandez, C. E.; Cohen, B.; Hare, P. M.; Kohler, B. *Chem. Rev.* (Washington, D.C.), 1977, *104*, 2004.
(5) (a) Sobolewski, A. L.; Domcke, W. *Chem. Phys.* **2000**, *259*, 181. (b) Sobolewski, A. L.; Domcke, W. *J. Phys. Chem. A* **2001**, *105*, 9275. (c) Sobolewski, A. L.; Domcke, W.; Dedonder-Lardeux, C.; Jouvet, C. *Phys. Chem. Chem. Phys.* **2002**, *4*, 1093. (d) Roos, B. O.; Malmqvist, P. A.; Molina, V.; Serrano-Andres, L.; Merchan, M. *J. Chem. Phys.* **2002**, *116*, 7526. (e) Vallet, V.; Lan, Z. G.; Mahapatra, S.; Sobolewski, A. L.; Domcke, W. *Faraday Discuss.* **2004**, *127*, 283. (f) Lan, Z. G.; Domcke, W.; Vallet, V.; Sobolewski, A. L.; Mahapatra, S. *J. Chem. Phys.* **2005**, *122*, 224315. (g) Vallet, V.; Lan, Z. G.; Mahapatra, S.; Sobolewski, A. L.; Domcke, W. *J. Chem. Phys.* **2005**, *123*, 144307. (h) Barbatti, M.; Vazdar, M.; Aquino, A. J. A.; Eckert-Maksic, M.; Lischka, H. *J. Chem. Phys.* **2006**, *125*, 164323. (i) Frank, I.; Damianos, K. *J. Chem. Phys.* **2007**, *126*, 125105.
(6) Blank, D. A.; North, S. W.; Lee, Y. T. *Chem. Phys.* **1994**, *187*, 35.
(7) (a) Wei, J.; Riedel, y, J.; Kuczmann, A.; Renth, F.; Temps, F. *Chem. Chem. Phys* **2003**, *5*, 315. (b) Wei, J.; Riedel, y.J.; Kuczmann, A.; Renth, F.; Temps, F *Faraday Discuss.* **2004**, *127*, 267. (c) Cronin, B.; Nix, M. G. D.; , R. H. Q.; Ashfold, M. N. R *Phys. Chem. Chem. Phys.* **2004**, *6*, 5031. (d) Cronin, B.; Devine, A. L.; Nix, M. G. D.; Ashfold, M. N. R. *Phys. Chem. Chem. Phys.* **2006**, *8*, 3440. (e) Cronin, B.; Nix, M. G. D.; Devine, A. L.; Dixon, R. N.; Ashfold, M. N. R. *Phys. Chem. Chem. Phys.* **2006**, *8*, 599. (f) Poterya, V.; Profant, V.; Farnik, M.; Slavicek, P.; Buck, U. *J. Chem. Phys.* **2007**, *127*, 064307.
(8) Tseng, C. M.; Lee, Y. T.; Ni, C. K. *J. Chem. Phys.* **2004**, *121*, 2459.
(9) Lin, M. F.; Tseng, C. M.; Lee, Y. T.; Ni, C. K. *J. Chem. Phys.* **2005**, *123*, 124303.
(10) (a) Nix, M. G. D.; Devine, A. L.; Cronin, B. *J. Chem. Phys.* **2006**, *125*, 133318. (b) Nix, M. G. D.; Devine, A. L.; Cronin, B.; Ashfold, M. N. R. *Phys. Chem. Chem. Phys.* **2006**, *8*, 2610.

(11) Borisevich, N. A.; Sukhodola, A. A.; Tolstorozhev, G. B. *J. Appl. Spectrosc.* **2007**, *74*, 379.
(12) Kajii, Y.; Obi, K.; Nkashima, N.; Yoshihara, K. *J. Chem. Phys.* **1987**, *87*, 5059.
(13) Ando, M.; Yoshiike, S.; Suzuki, T.; Ichimura, T.; Okutsu, T.; Ueda, M.; Horiuchi, H.; Hiratsuka, H.; Kawai, A.; Shibuya, K. *J. Photochem. Photobiol. A: Chem.* **2005**, *174*, 194.
(14) (a) Tsai, S. T.; Lin, C. K.; Lee, Y. T.; Ni, C. K. *Rev. Sci. Instrum.* **2001**, *72*, 1963. (b) Huang, C. L.; Lee, Y. T.; Ni, C. K. in *Modern Chemical Reaction Dynamics: Experiment and Theory;* Liu, K., Yang, X., Eds.; World Scientific Publisher: Singapore, 2004. (c) Ni, C. K.; Lee, Y. T. *Int. Rev. Phys. Chem.* **2004**, *23*, 2187.
(15) Tseng, C. M.; Lee, Y. T.; Lin, M. F.; Ni, C. K.; Liu, S. Y.; Lee, Y. P.; Xu, Z. F.; Lin, M. C. *J. Phys. Chem. A* **2007**, *111*, 9463.
(16) McDiarmid, R.; Xing, X. *J. Chem. Phys.* **1996**, *105*, 867.

JP8100305